Inorganica Chimica Acta 362 (2009) 2006–2014

Contents lists available at ScienceDirect

Inorganica Chimica Acta

journal homepage: www.elsevier.com/locate/ica

Synthesis and characterisation of new Schiff base metal complexes and their use as catalysts for olefin cyclopropanation

Nabil S. Youssef [a,*], Eman El-Zahany [a], Ahmed M.A. El-Seidy [a], Alessandro Caselli [b,*], Simone Fantauzzi [b], Sergio Cenini [b]

[a] Inorganic Chemistry Department, National Research Centre, Dokki, Giza, Egypt
[b] Dipartimento di Chimica Inorganica, Metallorganica e Analitica "Lamberto Malatesta", Università degli Studi di Milano, and ISTM-CNR;Via Venezian 21, 20133 Milan, Italy

ARTICLE INFO

Article history:
Received 6 May 2008
Received in revised form 3 September 2008
Accepted 10 September 2008
Available online 16 September 2008

Keywords:
Schiff bases
Metal complexes
Cyclopropanation
Homogeneus catalysis

ABSTRACT

New transition metal complexes of Co^{II}, Cu^{II}, Ni^{II} and $V^{IV}O$ with the Schiff base, HL, 3-acetylcoumarin-*N*(4)-phenylthiosemicarbazone have been prepared. Characterisation of the HL ligand and its complexes is also reported. Mass spectra and NMR assignments for the ligand, using COSY, NOESY homonuclear and HMQC and HMBC heteronuclear correlation techniques were carried out. Electronic and magnetic moments of the complexes indicate that the geometries of the metal centres are either distorted octahedral, square pyramidal, square planar or tetrahedral. The structures are consistent with the IR, UV–Vis, ESR, as well as conductivity and magnetic moments measurements. Cyclopropanation reactions of unactivated olefins by ethyldiazoacetate (EDA) in the presence of $LCu^{II}Cl$ as catalyst proceed with excellent TON (up to 9625).

1. Introduction

In the recent years, considerable attention has been given to the preparation of transition metal complexes of Schiff bases due to their interesting and important properties. Schiff bases represent a class of important compounds in medicinal and pharmaceutical field. They have biological activities such as antibacterial [1–4], anticancer [5–7], antifungal [8,9] and herbicidal activities [10]. Furthermore, Schiff bases offer opportunities for inducing substrate chirality, tuning metal centred electronic factors, enhancing solubility and stability of either homogeneous or heterogeneous catalyst [11–16]. For instance there are several studies on Schiff base copper(II) and cobalt(II) complexes used for asymmetric and enantioselective catalysis [17–24]. Based on the aforementioned properties for Schiff bases and their complexes, we report herein the synthesis and spectroscopic studies of the Schiff base ligand HL, 3-acetylcoumarin-*N*(4)-phenylthiosemicarbazone, (**1**) and its Co^{II}, Cu^{II}, Ni^{II} and $V^{IV}O$ complexes. ^{13}C NMR spectra were also obtained to determine the structure of the ligand. The catalytic activity of complexes $[L_2Co_2Cl_2]\cdot 2H_2O$ (**2**), $[LCo(OC(O)CH_3)]\cdot H_2O$ (**3**) and $LCu^{II}Cl$ (**5**) toward the decomposition of ethyl diazoacetate (EDA) in the presence of olefins to yield cyclopropane products has also been investigated. Although various methodologies are available today, the cycloaddition of carbenoids to C=C double bonds is practically the most important one to construct this class of compounds. Stereochemical control of these reactions, such as differentiation of the enantiotopic faces of the double bond or *cis–trans* selectivity imposed on the cyclopropanation reaction by the presence of a substituent at the carbenoid carbon are the main issues [25,26]. However, another issue of the cyclopropanation is the chemoselectivity of the reaction: very often catalysts that are fast in the activation of the approaching carbenoid, namely diazoacetates, give olefins derived by coupling reactions as major by products. Rarely metal complexes can give high selectivities in cyclopropanation reactions together with high turnover number (TON). We report here that $LCu^{II}Cl$ (**5**) is a competent catalyst for the cyclopropanation of olefins.

2. Experimental

2.1. Material

All the reagents employed for the preparation of the ligand and its complexes were of the best grade available and used without further purification. Unless otherwise stated, all catalytic tests were carried out under an atmosphere of purified dinitrogen using modified Schlenk techniques. Solvents employed were dried and distilled before use by standard methods. Benzene, cyclohexene and 1-octene were distilled over sodium, styrene and α-methyl styrene were distilled over calcium hydride and stored under dinitrogen.

---

* Corresponding authors. Tel.: +39 02 5031 4372; fax: +39 02 5031 4405.
E-mail addresses: nabilyoussef@hotmail.com (N.S. Youssef), alessandro.caselli@unimi.it (A. Caselli).

0020-1693/$ - see front matter © 2008 Elsevier B.V. All rights reserved.
doi:10.1016/j.ica.2008.09.012

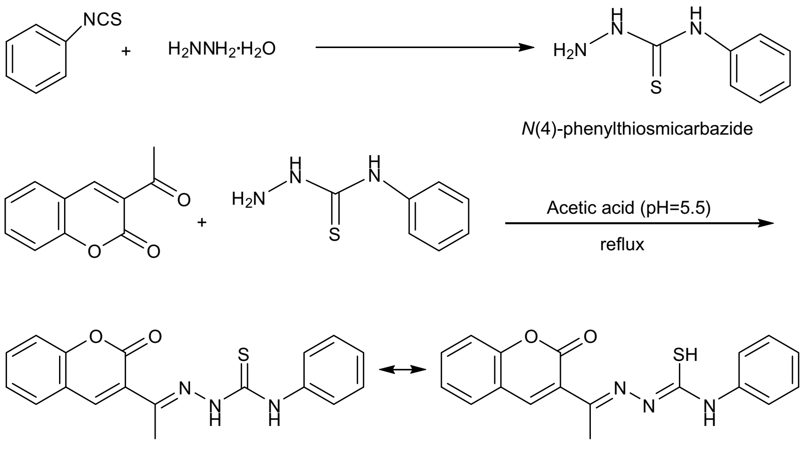

Scheme 1. Schematic representation for the formation of the Schiff base ligand HL (**1**).

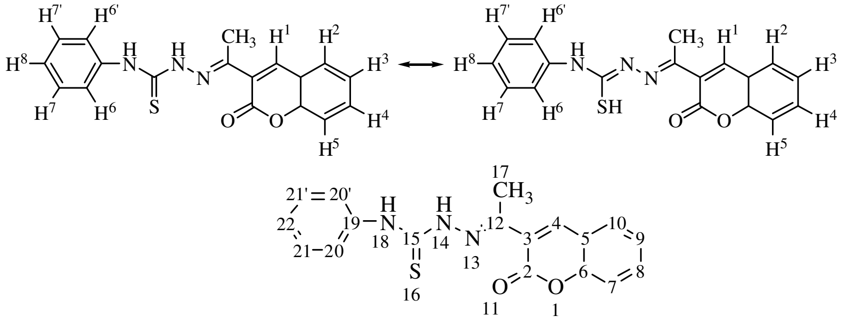

Chart 1. Numbering scheme for ligand HL (**1**).

2.2. Synthesis of the Schiff base ligand HL

The Schiff base ligand HL (**1**) was prepared in two steps. The reactions steps are illustrated in Scheme 1 (see Chart 1).

2.2.1. Synthesis of the N(4)-phenylthiosemicarbazide

N(4)-phenylthiosemicarbazide is prepared as reported in the literature. A solution of hydrazine hydrate (0.370 g, 7.397 mmol) in methanol (10 ml) was added dropwise to a stirred solution of phenylisothiocyanate (1.000 g, 7.397 mmol) in methanol (10 ml) at room temperature. A white precipitate starts to form immediately upon addition, the stirring was continued for 30 min, after which the white solid was filtered, washed with methanol and dried under vacuum over anhydrous $CaCl_2$ (97% yield).

2.2.2. Synthesis of the ligand, HL (*1*)

A few drops of glacial acidic acid were added to a hot solution (75 °C) of 3-acetyl-2*H*-chromen-2-one (1.125 g, 5.980 mmol) in ethanol (20 ml) and the mixture was then added to a hot solution (75 °C) of *N*(4)-phenylthiosemicarbazide (1.000 g, 5.980 mmol) in dioxane (10 ml). The reaction mixture was refluxed for 15 h. After cooling, water was added and a yellow precipitate started to form; the solid was filtered and washed with water then with ethanol. The product was re-crystallised from ethanol and dried under vacuum over anhydrous $CaCl_2$ (75% yield). ^{1}H NMR (300 MHz, DMSO): $\delta = 9.83$ (s, 1H, N*H*), 8.66 (s, 1H, H^1), 7.96 (d, $J = 8.4$ Hz, 1H, H^2), 7.76 (pst, $J = 8.4$ Hz, 1H, H^4), 7.55 (d, $J = 7.5$ Hz, 2H, H^6, $H^{6'}$), 7.47 (d, $J = 8.4$ Hz, 1H, H^5), 7.43 (pst, $J = 8.4$ Hz, 1H, H^3), 7.30 (pst, $J = 7.5$ Hz, 2H, H^7, $H^{7'}$), 6.94 (t, $J = 7.5$ Hz, 1H, H^8), 3.31 (s, S*H*) overlapping with H_2O, 2059 (s, 3H, CH_3). ^{13}C NMR (300 MHz, DMSO, 300 K): 196.0 C(3), 159.0 C(12), 155.5 C(6), 147.9 C(4), 141.0 C(18), 135.3 C(8), 131.6 C(10), 129.8 C(21) and C(21′), 125.8 C(9), 121.8 C(22), 117.6 C(20) and C(20′), 117.0 C(7) and 30.9 C(17).

2.3. Synthesis of the metal complexes

The metal complexes of the ligand HL (**1**) were prepared by mixing a hot methanolic solution of the metal chlorides: $CoCl_2 \cdot 6H_2O$, $CuCl_2 \cdot 2H_2O$, $NiCl_2 \cdot 6H_2O$, metal acetates: $Co(CH_3COO)_2 \cdot 4H_2O$, $Ni(CH_3COO)_2 \cdot 4H_2O$, $Cu(NO_3)_2$ or $VOSO_4 \cdot H_2O$ with the required amount of a hot ethanolic solution of the ligand to form 1:1 or 1:2 M/L (metal/ligand) complexes, or in the presence of 1,10-phenanthroline (Phen) as a secondary ligand, as shown in Table 1. The reaction mixture was then refluxed for a time depending on the transition metal salt used. Some complexes: **2**, **6** and **9** did not separate on standing but only when an aqueous KOH solution ($0.5\ \text{mol} \times \text{dm}^{-3}$) was added under stirring until the pH reached ~5.0. Formation of all complexes began with a change in the colour of the mixture. In the case of complex **5** instead of adding KOH solution, the solution was concentrated to half of its original volume before the formation of a green precipitate was observed. The precipitates formed were filtered, washed with ethanol, then with diethyl ether and dried under vacuum over anhydrous $CaCl_2$.

2.4. Physical measurements

The ligand and its metal complexes were analysed for C, H, N and M contents at the Microanalytical Laboratory, Faculty of Science, Cairo University, Egypt. Analytical and physical data of the ligand HL and its metal complexes are reported in Table 2. The metal ion contents of the complexes were also determined [27–29] by the

Table 1
Amounts of the reactants used in the formation of the metal complexes

No.	Complex	Metal salt used	Metal chloride, nitrate, acetate, or sulphate in 10–20 mL methanol		HL ligand in 10–25 mL ethanol		Phenanthroline (Phen) in 20 mL ethanol	
			Mass (g)	mmol	Mass (g)	mmol	Mass (g)	mmol
	1:1 M/L							
2	$[L_2Co_2Cl_2] \cdot 2H_2O$	$CoCl_2 \cdot 6H_2O$	0.476	2.0	0.676	2.0		
3	$[LCo(OC(O)CH_3)] \cdot H_2O$	$Co(CH_3COO)_2 \cdot 4H_2O$	0.499	2.0	0.676	2.0		
4	$[LVO(H_2O)]_2{\cdot}(SO_4) \cdot H_2O$	$VO(SO_4) \cdot H_2O$	0.361	2.0	0.675	2.0		
5	LCuCl	$CuCl_2 \cdot 2H_2O$	0.426	2.5	0.843	2.5		
6	$L_2Cu_2Cl_2(H_2O)_2$	$CuCl_2 \cdot 2H_2O$	0.426	2.5	0.843	2.5		
10	$LNi(OOCCH_3)$	$Ni(CH_3COO)_2 \cdot 4H_2O$	0.498	2.0	0.675	2.0		
	1:2 M/L							
7	$[L_2Cu] \cdot H_2O$	$Cu(NO_3)_2 \cdot 3H_2O$	0.256	1.5	1.013	3.0		
9	$[L_2Ni] \cdot 3H_2O$	$NiCl_2 \cdot 6H_2O$	0.316	1.3	0.897	2.7		
	1:1:1 M/L/Phen							
8	$[LCuCl(Phen)]{\cdot}2H_2O$	$CuCl_2 \cdot 2H_2O$	0.512	3.0	1.013	3.0	0.541	3.0

Table 2
Analytical and physical data of the ligand HL and its metal complexes

No.	Ligand/complexes	Colour	FW	Yield (%)	Anal./found (calc.) (%)				Molar conductance Λ_m (Ω^{-1} cm^2 mol^{-1})
					C	H	N	M	
1	HL	yellow	337.40	65	63.95 (64.08)	4.60 (4.48)	12.65 (12.45)		
2	$[L_2Co_2Cl_2] \cdot 2H_2O$	sap green	897.58	70	48.19 (48.17)	3.73 (3.59)	9.55 (9.36)	13.00 (13.13)	13
3	$[LCo(OC(O)CH_3)] \cdot H_2O$	brown	472.38	84	50.70 (50.85)	4.02 (4.05)	8.76 (8.90)	12.33 (12.48)	15
4	$[LVO(H_2O)]_2 \cdot (SO_4) \cdot H_2O$	green	478.38	67	44.99 (45.19)	3.50 (3.58)	8.63 (8.78)	10.57 (10.65)	110
5	LCuCl	green	435.39	94	49.49 (49.66)	3.12 (3.24)	9.51 (9.65)	14.45 (14.60)	11
6	$L_2Cu_2Cl_2(H_2O)_2$	brown	903.98	76	47.86 (47.68)	3.33 (3.56)	9.19 (9.27)	14.18 (14.02)	10
7	$[L_2Cu] \cdot H_2O$	brown	753.10	82	57.14 (57.32)	4.01 (4.01)	11.31 (11.14)	8.28 (8.42)	10
8	$[LCuCl(Phen)] \cdot 2H_2O$	brown	650.07	72	55.14 (55.30)	4.22 (4.02)	10.57 (10.75)	9.59 (9.75)	14
9	$[L_2Ni] \cdot 3H_2O$	beige	785.51	80	55.05 (55.04)	4.22 (4.36)	10.98 (10.70)	7.34 (7.47)	8
10	$LNi(OOCCH_3)$	ochre	454.12	81	52.64 (52.90)	3.73 (3.77)	9.36 (9.25)	12.67 (12.92)	17

previously reported methods [30,31]. IR spectra of the ligands and their metal complexes were measured using KBr discs with a Jasco FT/IR 300E Fourier transform infrared spectrophotometer covering the range 400–4000 cm^{-1} and in the 500–100 cm^{-1} region using polyethylene-sandwiched Nujol mulls on a Perkin Elmer FT-IR 1650 spectrophotometer. ^{1}H and ^{13}C NMR spectra were obtained on Brucker Avance 300-DRX or Avance 400-DRX spectrometers. Chemical shifts (ppm) are reported relative to TMS. The mass spectra were run at 70 eV with HP MODEL: MS. 5988A and/or GCMS. Cap 1000 EX SHIMADZU spectrometer using Electron Impact Technique. The electronic spectra of the ligands and their complexes were obtained in Nujol mulls and in saturated DMSO solutions using a Shimadzu UV–240 UV–Vis recording spectrophotometer. Molar conductivities of the metal complexes in DMSO (10^{-3} M) were measured using a dip cell and a Bibby conductimeter MC1 at room temperature. The resistance measured in ohms and the molar conductivities were calculated according to the equation: $\Lambda = V \times K \times M_w/g \times \Omega$, where Λ, molar conductivity (ohm^{-1} cm^2 mol^{-1}); V, volume of the complex solution (mL); K, cell constant 0.92 cm^{-1}; M_w, molecular weight of the complex; g, weight of the complex; and Ω, resistance measured in ohms. Magnetic moments at 298 K were determined using the Gouy method with $Hg[Co(SCN)_4]$ as calibrant. The solid ESR spectra of the complexes were recorded with ELEXSYS E500 Brucker spectrometer in 3-mm Pyrex Tubes at 298 K. Diphenylpicrylhydrazide (DPPH) was used as a g-marker for the calibration of the spectra. Mass spectra of the solid ligand were recorded using JEUL JMS-AX-500 mass spectrometer.

*2.5. Typical procedure for the catalytic cyclopropanation of olefins by LCu^{II}Cl (**5**)*

EDA (see caption of Tables 6 and 7 for quantities) was added to a suspension of LCu^{II}Cl (**5**) (5.0 mg, 1.15×10^{-2} mmol) and the olefin (see caption of Tables 6 and 7 for quantities) in 1,2-dichloroethane (10 mL). The resulting pale green solution was heated at the required temperature under stirring; depending on the olefin used and its concentration, after few minutes the solution turned to colourless and dinitrogen started to evolve from the system. The reaction was followed until total consumption of the EDA (IR absorbance, $\nu_{max} = 2114$ cm^{-1}, <0.025) was observed. The final solution was analysed by GC–MS after the addition of 2,4-dinitrotoluene as internal standard or evaporated to dryness under vacuum and products were separated by flash chromatography (eluant *n*-hexane/ethylacetate).

3. Results and discussion

3.1. Mass spectra of the ligand

The mass spectra of the Schiff base ligand HL (**1**) revealed the molecular ion peak at m/e 337, which is coincident with the formula weight (337.4) for this ligand and supports the identity of the structure. The pathway fragmentation pattern of the mass spectrum of the ligand is depicted in Scheme 2.

3.2. Infrared spectra of the complexes

IR spectra of the complexes were recorded to confirm their structures. The most characteristic vibrational frequencies and their tentative assignments for the ligand HL (**1**) and its transition metal complexes are listed in Table 3. The assignments were made by comparison with the vibrational frequencies of the free ligand.

The IR data obtained suggested that the ligand behaves as a mononegative tridentate ligand and coordinates through the C=N, C=O and C–S groups with displacement of one hydrogen

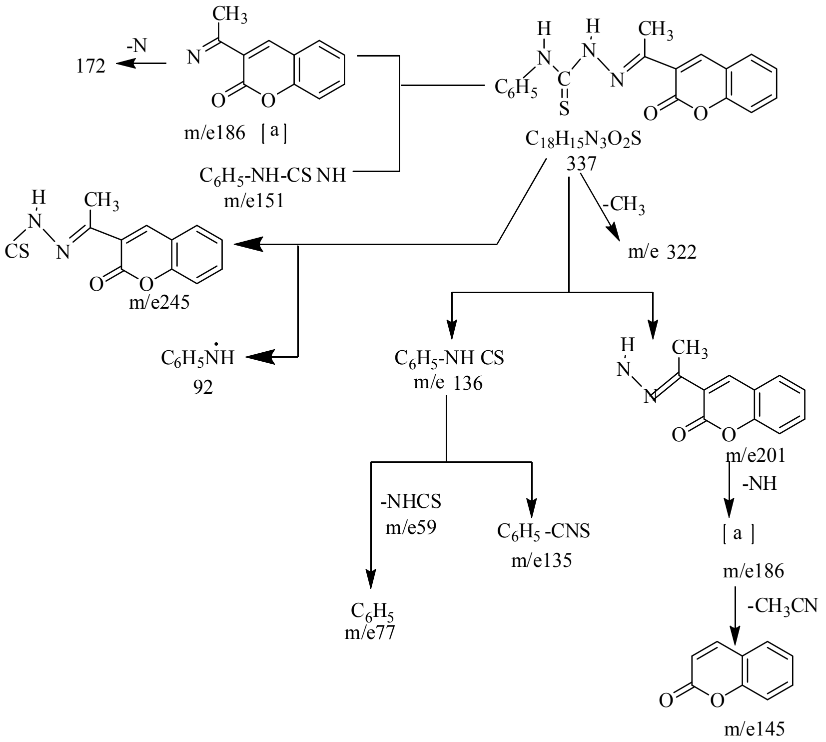

Scheme 2. Fragmentation pattern of the ligand HL (**1**).

Table 3
IR frequencies of the bands (cm^{-1}) of ligand HL (**1**) and its complexes and their assignments

No.	Compound	$\nu(OH/H_2O)$	$\nu(N^4H)$	$\nu(N^2H)$	$\nu(C{=}O)$	$\nu(C{=}S)$	$\nu(C{=}N)$	$\nu(N–N)$	$\nu(COO)$, s, as, $\Delta\upsilon$	$\nu(M–N)$	$\nu(M–S)$	$\nu(M–O)$
1	HL		3241 b	3197 m	1728 vs	871 s	1605 s	1116 s				
2	$[L_2Co_2Cl_2] \cdot 2H_2O$	3411 br	3283 s		1717 m		1600 m1620 m	1122 m		456 w	390 w	527 m
3	$[LCo(OC(O)CH_3)] \cdot H_2O$	3380 (br)	3295 w		1710 vw		1598 m 1650 w	1155 m	1558, 1315, $\Delta\upsilon = 243$	450 vw	355w	497 w
4	$[LVO(H_2O)]_2{\cdot}(SO_4) \cdot H_2O$	3401 br	3244 m		1715 vw		1605vw1625 m	1146 sh		460 m	395 m	530 m
5	LCuCl	3426 br	3270 sh		1710 w		1602 w1628 vw	1122 w		422 w	350w	505 w
6	$L_2Cu_2Cl_2(H_2O)_2$	3435 br	3287 m		1720 vw		1648 m1599 m	1120 w		445 w	340w	510 w
7	$[L_2Cu] \cdot H_2O$	3416 w	3290 sh		1714 m		1606 w1620 m	1134 w		450 w	345w	505 w
8	$[LCuCl(Phen)] \cdot 2H_2O$	3420 br	3248 m		1713 m		1550vw1614 m	1133 m		467 w	380 w	505 w
9	$[L_2Ni] \cdot 3H_2O$	3436 br	3212 w		1738 m		1603w1659 m	1122 m		455w	366 vw	486 w
10	$LNi(OOCCH_3)$	3421 br	3272 sh		1719 w		1600 m1654 m	1132 w	1532, 1435 $\Delta\upsilon = 97$	451 w	370w	493 w

atom upon enothiolization. In these complexes, the mode of coordination was suggested by the following evidences: (i) the disappearance of $\nu(N^2H)$, (ii) the shift of $\nu(C{=}N)$ to lower frequency together with its weak appearance (iii) the presence of a new band attributed to $\nu(C{=}N)$ [32] in the same spectral region for the $\nu(C{=}N)$ of the thiosemicarbazone moiety, (iv) the shift of $\nu(C{=}O)$ by 8–18 cm^{-1}, (v) the occurrence of the $\nu(N–N)$ band at higher wave numbers, (vi) the absence of the thioamide band (IV) [33] with the simultaneous appearance of new bands in the 340–390, 422–467, and 487–530 cm^{-1} regions due to the $\nu(M–S)$, $\nu(M–N)$ and $\nu(M–O)$ vibrations, respectively [34] (Chart 2).

The appearance of two characteristic bands in the ranges 1558–1495 cm^{-1} and 1435–1316 cm^{-1} in case of complexes **3** and **10** was attributed to $\nu_{asym.}(COO^-)$ and $\nu_{sym.}(COO^-)$, respectively, indicating the participation of the carboxylate oxygen in the complexes formation. The mode of coordination of carboxylate group has often been deduced from the magnitude of the observed separation between the $\nu_{asym.}(COO^-)$ and $\nu_{sym.}(COO^-)$. The separation value (Δ) between $\nu_{asym.}(COO^-)$ and $\nu_{sym.}$ in complex **3** was more than 200 cm^{-1} (243 cm^{-1}) suggesting the coordination of carboxylate group in a monodentate fashion [35]. The difference between the 1532 and 1435 cm^{-1} ($\Delta\nu = 97$ cm^{-1}) bands is correlated to the bidentate behaviour [36] in complex **10** (see Table 4).

The infrared spectrum of the sulphate complex **4** has bands at 1425 and 617 cm^{-1} characteristic for the uncoordinated sulphate group [37]. The IR spectrum of the VO(IV) complex display a band at 980 cm^{-1} assigned to the stretching frequency of the $\nu(V{=}O)$ [38].

The characteristic bands of 1,10-phenanthroline [35] appear at 1491, 1430, 830, and 694 cm^{-1} in the IR spectra of the ternary complex **8**, suggesting Phen coordination in this complex.

3.3. Molar conductance data

The metal complexes discussed herein were dissolved in DMF or DMSO and the molar conductivities of their solutions (10^{-3} M) at room temperature were measured to establish the charge of the metal complexes. The conductance data, reported in Table 2, indicated that all the metal complexes, except $[LVO(H_2O)]_2 \cdot (SO_4) \cdot H_2O$ (**4**), have conductivity values in the range characteristics for the non-electrolytic nature [39], suggesting that

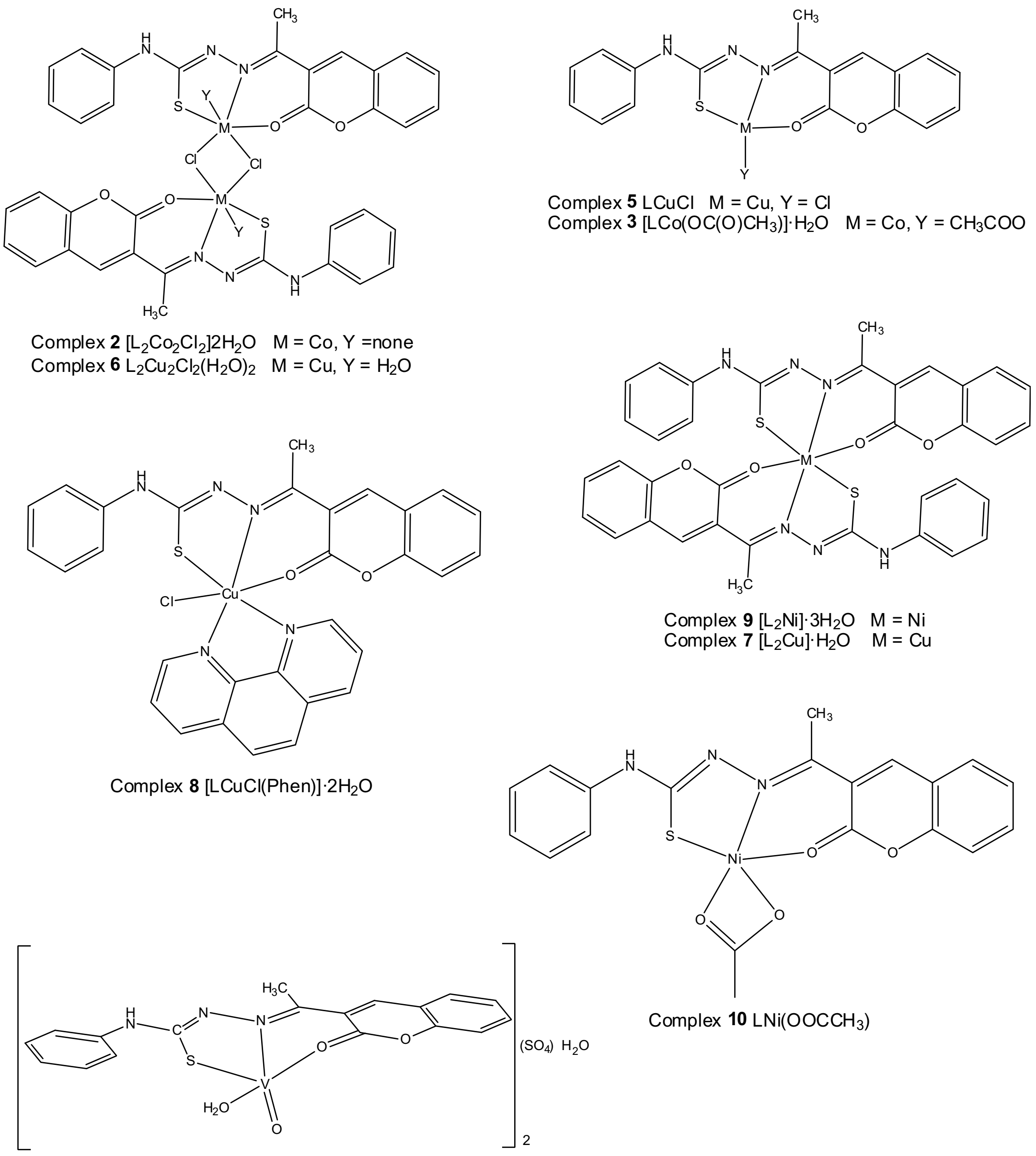

Complex **2** [$L_2Co_2Cl_2$]$2H_2O$ M = Co, Y = none
Complex **6** $L_2Cu_2Cl_2(H_2O)_2$ M = Cu, Y = H_2O

Complex **5** LCuCl M = Cu, Y = Cl
Complex **3** [LCo(OC(O)CH_3)]·H_2O M = Co, Y = CH_3COO

Complex **9** [L_2Ni]·$3H_2O$ M = Ni
Complex **7** [L_2Cu]·H_2O M = Cu

Complex **8** [LCuCl(Phen)]·$2H_2O$

Complex **10** LNi(OOCCH_3)

Complex **4**: [LVO(H_2O)]$_2$·(SO_4)H_2O

Chart 2. The proposed structures of metal complexes.

these complexes are neutral. On the other hand, the conductivity value of the complex **4** showed that it is electrolyte.

3.4. Electronic spectra and magnetic moments

3.4.1. Cobalt(II) complexes

The electronic spectrum for a square pyramidal d^7 configuration exhibits three transitions arising from the ground state $^4A_{1g}$ to higher excited states $^4B_{1g}(\nu_1)$, $^4E_g(\nu_2)$ and $^4A_{2g}(\nu_3)$ [40]. As the ν_1 band occurs at low energy, in the range not accessible due to instrumental limitations, it was not observed in the spectrum of complex **2**. The band observed for this complex at 680 nm may be due to the $^4A_{1g} \rightarrow {}^4E_g(\nu_2)$ transition, corresponding to a square pyramidal geometry. The highest band assigned to $^4A_{1g} \rightarrow {}^4E_g(\nu_2)$ transition was not observed due to overlapping with the more intense intraligand and charge transfer bands in the range 340–440 nm. The magnetic moment of complex **2** is 3.07, and indicates antiferromagnetic interaction between the adjacent metal ions in this binuclear complex. However, the dark brown [LCo(Ac)] · H_2O complex is four-coordinate and has magnetic susceptibility 2.2 B.M. suggesting considerable distortion toward a planar arrangement [41].

3.4.2. Copper(II) complexes

The magnetic moments of the copper complexes **7** and **8** at room temperature lie in the range 1.72–1.89 B.M. given in Table 6, corresponding to one unpaired electron and fall within the range observed for octahedral Cu(II) complexes [42]. This indicates that these complexes are monomeric in nature and there are no metal-metal interactions. The magnetic moment of complex **6** is 1.5 B.M., which is lower than the expected value for $\mu_{eff.}$ of a single Cu(II) ion in its octahedral complexes, thus it seems that there is antiferromagnetic exchange existing between Cu(II) ions in this complex. The electronic spectra of the copper complexes **6**, **7** and

Table 4
The electronic absorption spectral bands (nm) and magnetic moment (B.M.) for the ligand HL and its complexes

No.	Ligand/complex	Mode	π–π^*, n–π^* and CT bands	d–d bands	μ_{eff} in BM
1	HL	Nujol	280, 342.5, 380, 487.5		
2	$[L_2Co_2Cl_2] \cdot 2H_2O$	Nujol	270, 290, 350, 440	680	3.07
		DMSO	260, 300, 340		
3	$[LCo(OC(O)CH_3)] \cdot H_2O$	Nujol	260, 280, 450		2.2
		DMSO	257, 300, 455		
4	$[LVOH_2O]_2 \cdot H_2O \cdot (SO_4)$	Nujol	270, 350, 460	660, 790	1.73
		DMSO	265, 340, 470		
5	LCuCl	DMSO	275, 297, 315, 455	730	1.79
6	$L_2Cu_2Cl_2(H_2O)_2$	DMSO	260, 310, 425	680	1.5
7	$[L_2Cu] \cdot H_2O$	DMSO	260, 280, 330, 450	620	1.72
8	$[LCuCl(phen)] \cdot 2H_2O$	DMSO	258, 290, 305, 417	610	1.89
9	$[L_2Ni] \cdot 3H_2O$	DMSO	275, 350, 460	840	3.39
10	$LNi(OOCCH_3)$	DMSO	290, 380, 460	520, 700	3.87

8 show bands in the range of 680–610 nm assignable to $^2B_1\,g \rightarrow {}^2B_2\,g$ transition. This suggest that these complexes have tetragonal distorted octahedral geometry [43,44].

The presence of an absorption band at 730 nm in complex **5**, is presumably due to d–d transition. The green colour of this chelate confirms the distorted tetrahedral structure of this copper complex [45].

3.4.3. Nickel(II) complexes

$[L_2Ni] \cdot 3H_2O$, (**9**) is high spin with a magnetic moment value of 3.39 B.M., which is in the normal range observed for octahedral Ni(II) complexes. Its electronic spectrum displays a band at 840 nm which can be assigned to $^3A_{2g} \rightarrow {}^3T_{2g}$ transition, consistent with its octahedral stereochemistry [46].

$LNi(OOCCH_3)$, (**10**) shows recognizable bands at 700 and 520 nm. The positions of these spectral bands are consistent with those predicted for five coordinate Ni(II) complex [46]. These bands can be assigned respectively to $^3B_1 \rightarrow {}^3E$ and $^3B_1 \rightarrow {}^3A_2$ transitions assuming the effective symmetry to be C_{4v} [47].

3.4.4. Vanadyl complex

The electronic spectrum of this complex has two bands in the visible region at 790 and 520 nm, which are assigned to $^2B_2 \rightarrow {}^2E$ and $^2B_2 \rightarrow {}^2B_1$ transitions, respectively, as expected for a square pyramidal geometry in accordance with the Ballhausen–Gray scheme [48]. This complex exhibits magnetic moment due to its spin-only value of 1.73 B.M.

3.5. ESR Spectra

The X-band ESR spectra of the polycrystalline samples of the copper complexes are recorded at room temperature (298 K) and the data are given in Table 5. The spectra of all complexes are of axial shape with $g_{//} > g_{\perp}$ characteristic of complexes with $^2B_{1(dx2\text{-}y2)}$ orbital ground state. The average g values were calculated according to the equation $g_{av} = 1/3[g_{//} + 2\,g_{\perp}]$ and the results are given in Table 5. All complexes exhibit $g_{//} < 2.3$, suggesting covalent characters around the copper in present complexes. Kivelson and Neiman [49] have reported that a $g_{//}$ value greater than 2.3 indicates ionic character. The parameter G is calculated according to the equation $G = (g_{//} - 2.0023)/(g_{\perp} - 2.0023)$ and shows values >4. Data reported in Table 5, except in case of $L_2Cu_2Cl_2 \cdot (H_2O)_2$ complex (**6**), indicate that there is no direct copper-copper interaction in the solid state. In case of complex **6**, the G value is <4, which suggests considerable exchange interaction in this solid complex. The $g_{//}/A_{//}$ is taken as an indication for the stereochemistry of the copper(II) complexes. Addison [50] has suggested that this ratio may be an empirical indication of the tetrahedral distortion of the square planar geometry. The values of $g_{//}/A_{//}$ quotient in the range (105–135 cm) are expected for copper complexes within perfectly square based geometry and those higher than 150 cm for tetrahedrally distorted complexes. The values for the complexes under investigation, Table 5, showed that all complexes are associated with a tetrahedrally distorted field around the copper(II) centres.

Table 5
ESR parameters for copper(II) complexes

No.	Complex	$g_{//}$	g	$(g_{//})/(A_{//})$	G	$g_{av.}$
5	LCuCl	2.24	2.04628	161	5.4	
6	$L_2Cu_2Cl_2(H_2O)_2$	1.99	1.94		0.20	1.96
7	$[L_2Cu] \cdot H_2O$	2.2	2.04	214	5.24	2.1
8	$[LCuCl(Phen)] \cdot 2H_2O$	2.17	2.04	194	4.49	2.0

3.6. Catalytic activity

The catalytic activity of complexes $[L_2Co_2Cl_2] \cdot 2H_2O$ (**2**), $[LCo(OC(O)CH_3)] \cdot H_2O$ (**3**) and $LCu^{II}Cl$ (**5**) in cyclopropanation reactions has been investigated. As a model reaction we choose the cyclopropanation of α-methyl styrene by EDA (EDA = ethyl diazoacetate) (Scheme 3). Catalytic reactions were run by adding the EDA to a stirred solution containing the olefin and the metal complex in dichloroethane under dinitrogen.

Both cobalt complexes have a low catalytic activity as cyclopropanation catalyst and at 75 °C in 1,2-dichloroethane at a [Co]/EDA/olefin ratio of 1:100:400 we observed a conversion of less than 5% based on EDA after 2 h.

On the other hand, the copper complex $LCu^{II}Cl$ (**5**), exhibited an interesting catalytic capability toward the decomposition of ethyl diazoacetate, and the subsequent transfer of the carbene moiety to the C=C double bond. The condition of the catalytic reactions have been examined by changing the temperature, and the relative ratio [Cu]/EDA/olefin. Results are summarised in Table 6.

As it can be seen from data reported in Table 6, $LCu^{II}Cl$ is a very active catalyst for cyclopropanation reactions. A large excess of the olefin is not required for the reaction to proceed: even if equimolar amounts of EDA and olefin were used the cyclopropane products were obtained in reasonable yields (60%); the rest of the starting EDA is consumed to form the well-known coupling

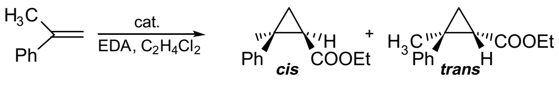

Scheme 3.

Table 6

Cyclopropanation of α-methyl styrene with EDA catalysed by $\mathrm{LCu^{II}Cl}$ (**5**)[a]

Entry	**5**/EDA/olefin	*T* (°C)	Time (min)	Conversion[b] (%)	Yield[c] (%)	*cis*:*trans*
1	1:100:100	60	39	>99	61.0	42:48
2		75	18	>99	60.0	44:56
3	1:100:200	R T	33	2		40:60
4		60	34	>99	72.2	41:59
5[d]		65	24/16/8	>99	72.7	47:53
6		75	11	>99	66.5	46:54
7	1:100:2000	60	35	>99	82.6	41:59
8		75	23	>99	84.6	46:54
9	1:200:400	60	29	>99	72.0	47:53
10		75	17	>99	66.8	46:54
11	1:200:2000	60	40	>99	86.8	42:58
12		75	22	>99	75.8	47:53
13	1:1000:2000	60	99	>99	77.8	46:54
14[e]	1:12500:25000	60	360	77	60.1	40:60

[a] Experimental conditions: EDA was added to a solution of LCuCl (**5**) (5.0 mg, 1.15×10^{-2} mmol) and α-methyl styrene in dichloroethane (10 mL).

[b] Conversion of the starting EDA.

[c] Determined by GC–MS (yield based on EDA).

[d] After complete consumption of the starting EDA, the catalytic cycle was restored twice by addition of EDA and α-methyl styrene; global yield is reported.

[e] LCuCl (**5**) (0.11 mg, 2.5×10^{-4} mmol) in dichloroethane (10 mL) were used. This solution was prepared by dissolving L(Cu)Cl (**5**) (1.1 mg, 2.53×10^{-3} mmol) in dichloroethane (100 mL).

by-products (maleate and fumarate) normally obtained in cyclopropanation reactions (Table 6, entries 1 and 2). The temperature plays an important role in these reactions: the catalyst at room temperature is inactive (Table 6, entry 3), but as soon as the temperature is increased to 60 °C it becomes very active. Reaction times can be almost reduced to a half just by increasing the temperature at 75 °C. After complete consumption of the starting EDA, the catalytic cycle can be restored just by addition of both reactants. In the second and third runs we observed even shorter reactions times (see later). The *cis*:*trans* ratio is not affected to a large extent by changing the conditions and nearly equal amounts of both cyclopropanes have always been obtained. The best result in terms of cyclopropane yield (86.8% based on EDA) was obtained at 60 °C at a **5**/EDA/olefin ratio of 1:200:2000 (Table 6, entry 11). In contrast to the prolonged EDA addition time generally required to reduce the formation of coupling products in cyclopropanation, we found complex **5** to be very active: a loading of 0.1 mol% of the catalyst and one pot addition of EDA completely consumed all the EDA and afforded cyclopropane products with good selectivity (77.7% based on EDA) in less than 100 min (TON 1000, Table 6, entry 13). The turnover number (TON) reached 9625 at a **5**/EDA/olefin ratio of 1:12550:25000 at 60 °C; in this case we observed a 77% conversion of the starting EDA in just 6 h (Table 6, entry 14).

Several alkenes were employed to determine the substrate scope of the complex $\mathrm{LCu^{II}Cl}$ (**5**) as cyclopropanation catalyst. At a **5**/EDA/olefin ratio of 1:100:200 at 75 °C, the complex catalysed the cyclopropanation of a range of substrates with quantitative conversion in short reaction times and with selectivities ranging from good to excellent. The results are summarised in Table 7.

When styrene is employed as substrate, we observed the quantitative conversion of the starting EDA in a comparable rate to what observed in the case of α-methyl styrene (compare entry 1, Table 7 and entry 6, Table 6). However, in this case the diastereoselectivity is improved (*cis*:*trans* = 33:67). Better yields in cyclopropane products, although with slightly longer reaction times, are obtained when electron-donating substituents are present in the *para* position of the aromatic ring (Table 7, entry 2). The same effect is observed when employing 4-chloro-α-methylstyrene as substrate (Table 7, entry 3). Even with these *para* substituted styrenes, the catalytic cycle can be restored just by addition of both reactants. In the second run and third run we observed even shorter reactions times. It can be seen that in the absence of an α-substituent on the styrene derivative the formation of the *trans* cyclopropane is slightly favored. Steric hindrance at the α position does not hamper the reaction and good yields are obtained even with 1,1-diphenyl ethylene (Table 7, entry 4). On the other hand, steric hindrance at the β-position of the styrene greatly affected the reactivities. *Trans*-β-methyl styrene gave lower reaction yields (55%) although with a good diastereoselectivity (Table 7, entry 7), whilst with *cis*-stilbene a dramatic drop in the cyclopropanation products was observed (Table 7, entry 6).

Even aliphatic double bonds that are generally less reactive towards cyclopropanation, gave excellent results. Though the time of the cyclopropanation reaction for these substrates increased slightly if compared to what observed for styrenic derivatives, very good yields were always obtained (Table 7, entries 8–11). Even in these cases *trans* cyclopropane compounds are obtained as major products and a remarkable diastereoselectivity (*trans*/*cis* = 11.5) has been observed in the case of cyclohexene (Table 7, entry 9). With 2,5-dimethyl-2,4-hexadiene, an important precursor to chrysanthemic acid [51], the catalytic reaction yielded the desired cyclopropanes in very good yields (91%) and with reasonable diastereoselectivities (Table 7, entry 10), without the need of a large excess of the olefin.

Copper(I) complexes are known to be more efficient cyclopropanation catalysts than copper(II) compounds. It has been observed that Cu(II) complexes are reduced to Cu(I) derivatives by the diazo compound under the reaction conditions. This has led to general agreement that the active catalyst is a Cu(I) species, irrespective of the oxidation state of the copper complex used as the precatalyst. It is also generally accepted that transition metal-catalysed cyclopropanation reactions proceed via a metal–carbene complex, which is formed by association of the diazo compound and the catalyst with concomitant extrusion of nitrogen [52]. Even if a detailed mechanistic study of the cyclopropanation reaction catalysed by complex $\mathrm{LCu^{II}Cl}$ (**5**) has not been undertaken yet, however, preliminary ^{1}H NMR experiments looking at the reaction of complex $\mathrm{LCu^{II}Cl}$ (**5**) (2 mg, 4.59×10^{-3} mmol) with EDA in the presence of α-methyl styrene, at a ratio [Cu]/EDA/olefin of 1:5:10 in $\mathrm{CDCl_3}$ (1 mL), showed the formation of a diamagnetic copper(I) complex during the reaction. Due to the very high reactivity of this complex, any attempt to isolate it met with failure. We can anyway note the following: (i) All the catalytic reactions tested need an induction period before the nitrogen evolution due to the EDA decomposition was observable. All the reactions were also followed by IR spectroscopy monitoring the disappearance of the band due to the stretching of the $\mathrm{N_2}$ moiety of the EDA ($\nu = 2114\ \mathrm{cm^{-1}}$). The consumption of the diazoacetate always started after an induction period. This explains why the catalytic cycle is faster in the second and third runs. This induction period depends also on the concentration of the olefin and increases with increasing the olefin concentration. (ii) When the EDA conversion reached completion, it was possible to restore the catalytic cycle just by adding new EDA and olefin to the reaction. In this case no induction period was necessary to the system and the reactions always proceeded to give cyclopropanes with almost identical yields. (iii) During the reaction the colour of the solution, due to the dissolved copper complex, changed from green (due copper(II) complex) to light yellow. The time needed for the change in colour was always coincident with the induction period. (iv) The induction period observed depends also on the olefin employed and longer times are observed for *trans*-β-methyl styrene or non conjugated double bonds (see also Table 7). (v) If the reaction is run in the air, longer reaction times are needed and we

Table 7
Cyclopropanation of olefins with EDA catalysed by $LCu^{II}Cl$ (**5**)[a]

Entry	Olefin	Time (min)	Conversion[b] (%)	Yield[c] (%)	*cis:trans*[c]
1	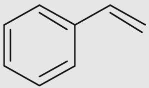	12	>99	59	33:67
2[d]	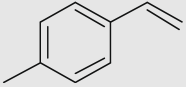	18/12/7	>99	87	34:66
3[d]	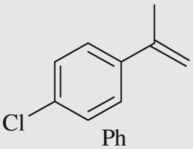	15/7/7	>99	87	49:51
4	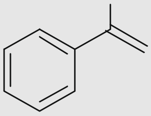	16	>99	68	
5	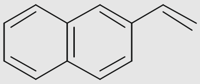	24	>99	56	29:71
6	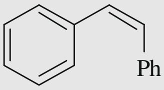	15	>99	2.0	39:63
7	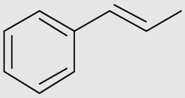	19	>99	55	28:72
8	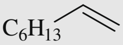	22	>99	70	31:69
9	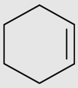	25	>99	83	8:92
10	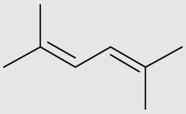	21	>99	91	35:65
11[e]	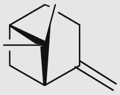	18	>99	84	59:40:1

[a] Experimental conditions: EDA was added to a solution of LCuCl (**5**) (5.0 mg, 1.15×10^{-2} mmol) and olefin in dichloroethane (10 mL) at 75 °C.
[b] Conversion of the starting EDA.
[c] Determined by GC–MS (yield based on EDA).
[d] After complete consumption of the starting EDA, the catalytic cycle was restored twice by addition of EDA and olefin; global yield is reported.
[e] Only three products out of four possible diastereoisomers were detected by GC–MS.

never obtained a full conversion of the starting EDA in these cases.

All this data, together with the data reported in literature [53], suggest that the catalyst is activated during the induction period and that the initial reduction of copper(II) to copper(I) is necessary to the catalysis to take place.

4. Conclusions

The straightforward synthesis of the new Schiff base, HL, 3-acetylcoumarin-*N*(4)-phenylthiosemicarbazone has been reported. Its metal complexes with transition metals have been characterised and all the data collected are in agreement with the proposed structures. The spectral data indicate that the ligand can behave as monobasic tridentate ligand and coordinates through the C=N, C=O and C–S groups with displacement of one hydrogen atom upon enothiolization.

The monomeric copper(II) complex, $LCu^{II}Cl$, showed excellent catalytic activity in cyclopropanation reaction and we have reported that TON up to 9625 can be obtained. In contrast to the prolonged EDA addition time generally required to reduce the formation of coupling products in cyclopropanation, we found this complex to be very active and one pot addition of EDA is allowed to yield the desired cyclopropanes with excellent selectivity. Moreover the catalyst is very robust and no decrease in yield was observed even after three catalytic runs.

References

[1] F.D. Karia, P.H. Parsania, Asian J. Chem. Soc. 11 (1999) 991.
[2] P.G. More, R.B. Bhalvankar, S.C. Pattar, J. Indian Chem. Soc. 78 (2001) 474.
[3] A.H. El-Masry, H.H. Fahmy, S.H.A. Abdelwahed, Molecules 5 (2000) 1429.
[4] M.A. Baseer, V.D. Jadhav, R.M. Phule, Y.V. Archana, Y.B. Vibhute, Orient. J. Chem. 16 (2000) 553.
[5] S.B. Desai, P.B. Desai, K.R. Desai, Heterocycl. Commun. 7 (2001) 83.
[6] E.M. Hodnett, W.J. Dunn, J. Med. Chem. 13 (1970) 768.
[7] P. Pathak, V.S. Jolly, K.P. Sharma, Orient. J. Chem. 16 (2000) 161.
[8] S.N. Pandeya, D. Sriram, G. Nath, E.D. Clercq, Il Farmaco 54 (1999) 624.
[9] W.M. Singh, B.C. Dash, Pesticides 22 (1988) 33.
[10] S. Samadhiya, A. Halve, Orient. J.Chem. 17 (2001) 119.
[11] B.D. Clercq, F. Verpoort, Macromolecules 35 (2002) 8943.
[12] T. Opstal, F. Verpoort, Synlett 6 (2002) 935.
[13] T. Opstal, F. Verpoort, Angew. Chem., Int. Ed. 42 (2003) 2876.
[14] S.N. Pal, S. Pal, Inorg. Chem. 40 (2001) 4807.
[15] B.D. Clercq, F. Verpoort, Adv. Synth. Catal. 34 (2002) 639.
[16] B.D. Clercq, F. Lefebvre, F. Verpoort, Appl. Catal. A247 (2003) 345.
[17] Z. Li, G.L.Z. Zheng, H. Chen, Tetrahedron 56 (2000) 7187.
[18] L. Cai, H. Mahmoud, Y. Han, Tetrahedron: Asymmetry 10 (1999) 411.
[19] C.-M. Che, H.-L. Kwong, W.-C. Chu, K.-F. Cheng, W.-S. Lee, H.-S. Yu, C.-T. Yeung, K.-K. Cheung, Eur. J. Inorg. Chem. (2002) 1456.
[20] H.B. Zhu, Z.Y. Dai, W. Hung, K. Cui, S.H. Gou, C.J. Zhu, Polyhedron 23 (2004) 1131.
[21] K.M. Gillespie, C.J. Sanders, P. O'Shaughnessy, I. Westmoreland, C.P. Thickitt, P. Scott, J. Org. Chem. 67 (2002) 3450.
[22] T. Nagata, K. Yorozu, T. Yamada, T. Mukaiyama, Angew. Chem., Int. Ed. 34 (1995) 2145.
[23] E.N. Jacobsen, W. Zhang, M.L. Guler, J. Am. Chem. Soc. 113 (1991) 6703.
[24] G.L. Estiu, A.H. Jubert, J. Costamagna, J. Vargas, Inorg. Chem. 35 (1996) 263.
[25] H. Lebel, J.-F. Marcoux, C. Molinaro, A.B. Charette, Chem. Rev. 103 (2003) 977.
[26] H. Pellissier, Tetrahedron 64 (2008) 7041.
[27] F.J. Welcher, The Analytical Use Of EDTA, Van Norstrand, USA, 1958.
[28] A.I. Vogel, A Text Book of Quantitative Inorganic Analysis, fourth ed., Longman, London, 1978.
[29] Z. Holzbecher, L. Divis, M. Kral, L. Sucha, F. Vlacil, Hand book of Organic Reagents in Inorganic Analysis, John Wiley, New York, 1976.
[30] A.M.G. Macdonald, P. Sirichanya, Microchem. J. 14 (1969) 199.
[31] N.S. Youssef, Synth. React. Inorg. Met.-Org. Chem. 30 (2000) 225.
[32] V. Philip, V. Suni, M.R. Prathapachandra Kurup, M. Nethaji, Polyhedron 25 (2006) 1931.
[33] R.P. John, A. Sreekanth, M.R.P. Kurup, S.M. Mobin, Polyhedron 21 (2002) 2515.
[34] K.H. Reddy, P.S. Reddy, Transition Met. Chem. 25 (2000) 505.
[35] D.M. Boghaei, M. Gharagozlou, Spectrochim. Acta 67A (2007) 944.
[36] R.M. El-Shazly, G.A.A. Al-Hazmi, S.E. Ghazy, M.S. El-Shahawi, A.A. El-Asmy, Spectrochim. Acta A61 (2005) 243.
[37] S. Chandra, L.K. Gupta, Spectrochim. Acta, Part A A61 (2005) 2549.
[38] A.A.A. Emara, A.A. Saleh, O.M.I. Adly, Spectrochim. Acta, Part A 68 (2007) 592.
[39] A. Golcu, M. Tumer, H. Demirelli, R.A. Wheatley, Inorg. Chim. Acta 358 (2005) 1785.
[40] S. Tascioglu, O. Buyukgungor, A. Aydin, A.K. Medjidov, Polyhedron 25 (2006) 1279.
[41] K.A. Ketcham, J.K. Swearingen, A. Castineiras, I. Garcia, E. Bermejo, D.X. West, Polyhedron 20 (2001) 3265.
[42] G.G. Mohamed, N.E.A. El-Gamel, Spectrochim. Acta, Part A A60 (2004) 3141.
[43] S. Chandra, Sangeetika, Spectrochim. Acta, Part A 60 (2004) 2153.
[44] N.M. Shauib, A.-Z.A. Elassar, A. El-Dissouky, Spectrochim. Acta, Part A 63 (2006) 714.
[45] R.N. Jedeja, N.J. Parmar, Synth. React. Inorg. Met.-Org. Chem. 35 (2005) 111.
[46] S. Chandra, U. Kumar, Spectrochim. Acta, Part A 61 (2005) 219.
[47] G.G. Mohamed, Spectrochim. Acta, Part A 64 (2006) 188.
[48] U.B. Gangadharmath, S.M. Annigeri, A.D. Naik, V.K. Revankar, V.B. Mahale, J. Mol. Struct. 572 (2001) 61.
[49] D. Kivelson, R. Neiman, J. Chem. Phys. 35 (1961) 149.
[50] A.W. Addison, in: K.D. Karlin, J. Zubieta (Eds.), Copper Coordination Chemistry Biochemical and Inorganic Perspectives, Adenine Press, New York, 1983.
[51] M. Itagaki, K. Suenobu, Org. Process Res. Dev. 11 (2007) 509.
[52] J.M. Fraile, J.I. Garcia, V. Martinez-Merino, J.A. Mayoral, L. Salvatella, J. Am. Chem. Soc. 123 (2001) 7616.
[53] R.L. Safiullin, V.A. Dokichev, L.R. Yakupova, R.M. Sultanova, S.L. Khurasan, R.N. Zaripov, Y.U.V. Tomilov, Kinet. Catal. 49 (2008) 43.